Adenosine Triphosphate–dependent Asymmetry of Anion Permeation in the Cystic Fibrosis Transmembrane Conductance Regulator Chloride Channel

PAUL LINSDELL and JOHN W. HANRAHAN

From the Department of Physiology, McGill University, Montréal, Québec, Canada H3G 1Y6

ABSTRACT The cystic fibrosis transmembrane conductance regulator (CFTR) forms a tightly regulated channel that mediates the passive diffusion of Cl^- ions. Here we show, using macroscopic current recording from excised membrane patches, that CFTR also shows significant, but highly asymmetrical, permeability to a broad range of large organic anions. Thus, all large organic anions tested were permeant when present in the intracellular solution under biionic conditions ($P_X/P_{Cl} = 0.048$–0.25), whereas most were not measurably permeant when present in the extracellular solution. This asymmetry was not observed for smaller anions. ATPase inhibitors that "lock" CFTR channels in the open state (pyrophosphate, 5′-adenylylimidodiphosphate) disrupted the asymmetry of large anion permeation by allowing their influx from the extracellular solution, which suggests that ATP hydrolysis is required to maintain asymmetric permeability. The ability of CFTR to allow efflux of large organic anions represents a novel function of CFTR. Loss of this function may contribute to the pleiotropic symptoms seen in cystic fibrosis.

KEY WORDS: anion permeation • anion selectivity • chloride channel • ATPase • cystic fibrosis

INTRODUCTION

Cystic fibrosis is caused by mutations in a single gene, that encoding the cystic fibrosis transmembrane conductance regulator (CFTR)[1] (Riordan et al., 1989). CFTR is a member of the ATP-binding cassette (ABC) family of membrane proteins, most members of which are thought to form ATP-dependent pumps of a wide range of substances (Higgins, 1995; Tusnády et al., 1997). In contrast, CFTR is a phosphorylation- and ATP-dependent ion channel that mediates the passive electrodiffusion of Cl^- ions (see Gadsby et al., 1995; Hanrahan et al., 1995). It remains unclear how the reduced epithelial Cl^- conductance caused by the functional absence of CFTR leads to the complex symptoms seen in cystic fibrosis lung disease.

Previously, we described the permeation properties of CFTR at the single channel level (Tabcharani et al., 1997; Linsdell et al., 1997*a*, 1997*b*). Selectivity among smaller anions showed a lyotropic sequence, suggesting that anion permeability is dominated by ionic hydration energies. The permeability to larger anions suggested a minimum functional pore diameter of ~5.3 Å. However, since sparingly permeant anions may carry unitary currents that are too small to be resolved by single channel recording, this value is likely to be an underestimate. Here we report a more extensive examination of CFTR permeation using macroscopic current recording from membrane patches that contain hundreds of CFTR channels (see Linsdell and Hanrahan, 1996*a*). Using this more sensitive recording technique, we found that a wide range of large, organic anions are slightly permeant in CFTR, but only when present in the intracellular solution; these same ions were not measurably permeant when present in the extracellular solution. This strong asymmetry in large anion permeability was dependent on ATP hydrolysis, since ATPase inhibitors stimulated influx of large anions from the extracellular solution, equalizing permeability to these anions measured when they were present in the intracellular or extracellular solution. As well as demonstrating a unique ATP dependence of CFTR anion selectivity, these results suggest a novel function for CFTR in providing an efflux pathway for large organic anions.

METHODS

Experiments were carried out on baby hamster kidney (BHK) or Chinese hamster ovary (CHO) cells stably expressing either wild-type or mutant (K335E or R347D) CFTR (Tabcharani et al., 1991, 1993; Linsdell and Hanrahan, 1996*a*). BHK cells were used for macroscopic current recording and CHO cells for single channel recording; BHK cells express a much higher density of CFTR channels after transfection with the pNUT-CFTR vector

Address correspondence to Paul Linsdell, Department of Physiology, McGill University, 3655 Drummond Street, Montréal, Québec, H3G 1Y6, Canada. Fax: 514-398-7452; E-mail: linsdell@physio.mcgill.ca

[1]*Abbreviations used in this paper:* ABC, ATP-binding cassette; AMP-PNP, 5′-adenylylimidodiphosphate; BHK, baby hamster kidney; CFTR, cystic fibrosis transmembrane conductance regulator; DNDS, 4,4′-dinitrostilbene-2,2′-disulfonic acid; *I*-V, current–voltage; PPi, pyrophosphate.

J. GEN. PHYSIOL. © The Rockefeller University Press • 0022-1295/98/04/601/14 $2.00
Volume 111 April 1998 601–614
http://www.jgp.org

(Seibert et al., 1995) and are therefore better suited to macroscopic current recordings. The permeation properties of CFTR are not expected to be influenced by the cell type in which they are expressed.

Macroscopic and single channel CFTR current recordings were both made using the excised, inside-out configuration of the patch clamp technique, as described previously (Linsdell and Hanrahan, 1996*a*; Linsdell et al., 1997*a*). Pipettes were fabricated using an upright two-stage puller (PP-83; Narishige Instruments, Tokyo, Japan). Pipettes used for macroscopic current recordings had resistances of 1–3 MΩ when filled with standard NaCl solution (see below), compared with 3–4 MΩ for pipettes used for single channel recordings. Channels were activated by exposure of the cytoplasmic face of the patch to 40–180 nM PKA plus 1 mM Mg · ATP. All macroscopic current–voltage relationships shown have had the background (leak) current recorded before addition of PKA digitally subtracted as described previously (Linsdell and Hanrahan, 1996*a*) and illustrated in Figs. 3 and 5. Leak currents were very small compared with the PKA-stimulated CFTR currents (<15%; see Figs. 3 and 5), and are not expected to affect the accuracy of the results. Furthermore, current returned to the same level after removal of PKA and ATP, indicating that the leak did not change over the course of the experiment (Figs. 3 and 5). No PKA-stimulated currents were observed in patches excised from control, untransfected BHK cells under any ionic conditions studied (for example, see Fig. 3 *D*). Current traces were filtered at 100 Hz (for macroscopic currents) or 50 Hz (for single channel currents) using an eight-pole Bessel filter, digitized at 250 Hz and analyzed using PCLAMP6 computer software (Axon Instruments, Foster City, CA). Current traces for variance analysis (see below) were filtered at 500 Hz and digitized at 1 kHz.

Most solutions contained (mM): 150 NaCl, 2 $MgCl_2$, 10 TES, or 154 NaX (where X is the anion being tested; see Table I for a list of anions used), 2 $Mg(OH)_2$, 10 TES; these solutions were adjusted to pH 7.4 with NaOH. To examine the permeability of zwitterionic pH buffers (HEPES, TES), the pH was adjusted to 9.0 to ensure that >95% of these molecules were in the anionic form. In these cases, solutions contained 154 mM NaCl, Na · HEPES, or Na · TES plus 1 mM Tris base. In some cases (see Fig. 2), NaCl or Na · gluconate were partly replaced in an isosmotic manner by sucrose; solutions therefore contained up to 231 mM sucrose. Although such a high concentration of sucrose in the intracellular solution causes a significant reduction in CFTR conductance (Linsdell and Hanrahan, 1996*b*), it is not expected to alter the current reversal potential. Where the pipette solution did not contain Cl^-, the pipette Ag/AgCl wire was protected by a NaCl-containing agar bridge inside the pipette. The bath agar bridge had the same composition as the pipette solution or the agar bridge in the pipette when one was necessary. Experiments with different anions were carried out on different patches. Voltages were corrected for measured liquid junction potentials of up to 12 mV existing between dissimilar pipette and bath solutions. All chemicals were obtained from Sigma Chemical Co. (St.

TABLE I

Apparent Permeability Ratios for Different Anions in CFTR

Anion	P_X/P_{Cl} (inside)	P_X/P_{Cl} (outside)	Ion dimensions
			Å
Thiocyanate	2.63 ± 0.13 (6)	2.26 ± 0.19 (4)	3.60 × 3.60 × 3.60
Nitrate	1.53 ± 0.04 (7)	1.35 ± 0.03 (4)	3.10 × 4.76 × 5.17
Bromide	1.23 ± 0.03 (5)	1.29 ± 0.01 (4)	3.90 × 3.90 × 3.90
Chloride	1.00 ± 0.01 (10)		3.62 × 3.62 × 3.62
Iodide	0.84 ± 0.03 (5)	0.24 ± 0.03 (5)	4.32 × 4.32 × 4.32
Fluoride	0.070 ± 0.002 (7)	0.021 ± 0.003 (5)	2.72 × 2.72 × 2.72
Formate	0.25 ± 0.01(8)	0.12 ± 0.01 (4)	3.40 × 4.62 × 4.82
Acetate	0.090 ± 0.004 (8)	0.036 ± 0.006 (4)	3.99 × 5.18 × 5.47
Perchlorate	0.25 ± 0.02 (6)	0.049 ± 0.006 (5)	4.63 × 4.64 × 4.91
Propanoate	0.14 ± 0.01 (4)	0.021 ± 0.002 (4)	4.12 × 5.23 × 7.05
Benzoate	0.069 ± 0.006 (6)	<0.014 (4)	3.55 × 6.30 × 8.57
Pyruvate	0.10 ± 0.01 (5)	<0.010 (4)	4.09 × 5.73 × 6.82
Hexafluorophosphate	<0.019 (4)		4.92 × 4.98 × 5.16
Methane sulfonate	0.077 ± 0.005 (5)	<0.010 (3)	5.08 × 5.43 × 5.54
Glutamate	0.096 ± 0.008 (4)		4.67 × 6.52 × 10.78
Isethionate	0.13 ± 0.01 (4)		5.35 × 5.79 × 7.60
Gluconate	0.071 ± 0.003 (54)	<0.013 (36)	4.91 × 6.86 × 12.09
Glucoheptonate	0.095 ± 0.005 (4)		5.50 × 6.51 × 13.54
Glucuronate	0.13 ± 0.02 (4)	<0.012 (4)	5.23 × 7.73 × 9.43
MES	0.13 ± 0.01 (4)		6.00 × 6.99 × 9.65
Galacturonate	0.079 ± 0.012 (5)	<0.013 (4)	6.51 × 6.66 × 8.10
HEPES (pH 9.0)	0.092 ± 0.012 (5)		6.64 × 6.64 × 12.86
TES (pH 9.0)	0.099 ± 0.012 (4)		6.63 × 6.75 × 11.35
Lactobionate	0.048 ± 0.008 (5)	<0.012 (5)	7.57 × 9.32 × 13.11

Relative permeabilities (P_X/P_{Cl}) of different anions, when present in the intracellular or extracellular solution under biionic conditions, were calculated from macroscopic current reversal potentials (Fig. 1, *A* and *B*) as described in METHODS. Numbers in parentheses indicate the number of patches examined for each ion. Minimum unhydrated ionic dimensions were estimated as described in METHODS. Maximum permeabilities are given for ions that were not measurably permeant over the voltage range used.

Louis, MO), except $NaClO_4$, $NaPF_6$, Na · benzoate, and Na · methane sulfonate (Aldrich Chemical Co., Milwaukee, WI), 4,4′-dinitrostilbene-2,2′-disulfonic acid (DNDS; Pfaltz and Bauer, Waterbury, CT), glibenclamide (glyburide; Calbiochem Corp., La Jolla, CA), and PKA (prepared in the laboratory of Dr. M.P. Walsh, University of Calgary, Calgary, Alberta, Canada, as described previously; Tabcharani et al., 1991).

Macroscopic current–voltage relationships were constructed using depolarizing voltage ramp protocols, with a rate of change of voltage of 37.5–75 mV/s (see Linsdell and Hanrahan, 1996*a*, and Figs. 3 and 5). The current reversal potential, E_{REV} was estimated by fitting a polynomial function to the current–voltage relationship, and was used to estimate permeability ratios according to the equation:

$$P_X/P_{Cl} = ([Cl]/[X]) \exp(-\Delta E_{REV} F/RT), \quad (1)$$

where ΔE_{REV} is the difference between the reversal potential observed with a test anion X and that observed with symmetrical Cl^-, and *F*, *R*, and *T* have their normal thermodynamic meanings.

To estimate the functional diameter of the narrowest part of the pore (see Fig. 1, *C* and *D*), the pore was modeled as a cylinder permeated by cylindrical-shaped ions (Linsdell et al., 1997*b*). Permeability ratios are then related to ion diameter according to an "excluded volume effect" (Dwyer et al., 1980):

$$P_X/P_{Cl} = k[1 - (a/d)]^2, \quad (2)$$

where *a* is the unhydrated diameter of the ion, *d* is the functional diameter of the pore, and *k* is a proportionality constant. Ion diameters were estimated as the geometric mean of the two smaller unhydrated ionic dimensions (given in Table I), estimated from space-filling models using Molecular Modeling Pro computer software (WindowChem Software Inc., Fairfield, CA) as described previously (Linsdell et al., 1997*b*).

Measurements of current variance were made during the slow activation of macroscopic current by low concentrations of PKA (see Fig. 6). Mean current and current variance were calculated for 5-s subrecords filtered at 500 Hz, giving a bandwidth of 0.2–500 Hz. The length of subrecords was chosen to minimize the error due to current activation during each subrecord without omitting too much of the low frequency variance. Variance-vs.-mean current relationships (see Figs. 6 and 7, *C* and *D*) were fitted by the equation (Sigworth, 1980):

$$\sigma^2_I = iI - (I^2/n) \quad (3)$$

where σ^2_I is the current variance, *I* the mean current, *i* the unitary current, and *n* the total number of channels.

Experiments were carried out at room temperature (21–23°C). Throughout, mean values are presented as mean ± SEM. For graphical presentation of mean values, error bars represent ±SEM; where no error bars are shown, ±SEM is smaller than the size of the symbol.

RESULTS

Lyotropic Selectivity Sequence of Macroscopic CFTR Currents

The ionic selectivity of macroscopic currents mediated by CFTR channels was examined using large, inside-out membrane patches excised from baby hamster kidney cells stably expressing a high density of CFTR channels

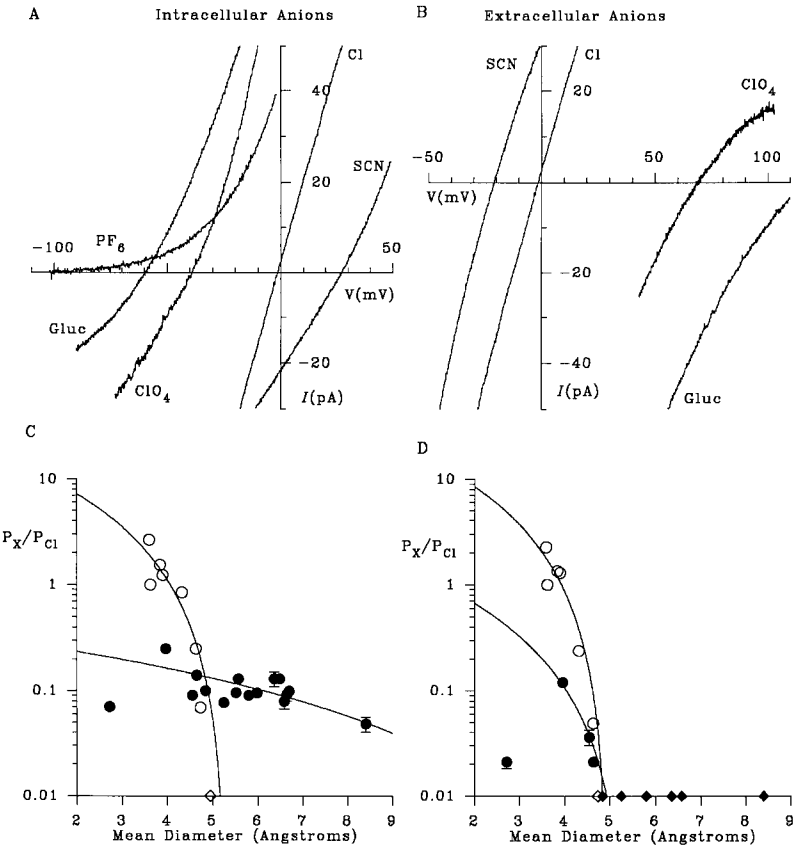

FIGURE 1. Selectivity of macroscopic CFTR currents. (*A*) Example *I-V* curves recorded with NaCl in the extracellular (pipette) solution and NaCl, NaSCN, $NaClO_4$, Na · gluconate (Gluc) or $NaPF_6$ (hexafluorophosphate) in the intracellular (bath) solution. (*B*) Example *I-V* curves with NaCl in the intracellular solution and NaCl, NaSCN, $NaClO_4$, or Na · gluconate in the extracellular solution. (*C* and *D*) Apparent permeability ratios for different intracellular (*C*) or extracellular (*D*) ions (P_X/P_{Cl}; taken from Table I) as a function of mean unhydrated ionic diameter. Open symbols represent lyotropic (weakly hydrated) ions (from left to right: SCN^-, Cl^-, NO_3^-, Br^-, I^-, ClO_4^-, benzoate, PF_6^-), and filled circles represent kosmotropic (strongly hydrated) ions (from left to right: fluoride, formate, acetate, propanoate, pyruvate, methane sulfonate, glutamate, isethionate, gluconate, glucoheptonate, glucuronate, MES, galacturonate, HEPES, TES, lactobionate) (see Collins, 1997). Ions that were not measurably permeant are shown as diamonds on the abscissa for display purposes only. In each case, the data have been fitted by Eq. 2 (see METHODS), giving estimates of the functional pore diameter of 5.3 (*C*, ○), 13.8 (*C*, ●), 4.9 (*D*, ○) and 5.3 (*D*, ●) Å.

(Linsdell and Hanrahan, 1996*a*). PKA-stimulated current–voltage (*I*-V) relationships were obtained with different anions bathing the intracellular (Fig. 1 *A*) or extracellular (Fig. 1 *B*) side of excised patches (see METHODS). Chloride solution was present on the opposite side of the membrane (i.e., biionic conditions). Reversal (zero-current) potentials determined from these curves were used to calculate apparent permeability ratios for each anion (P_X/P_{Cl}) according to Eq. 1 (see METHODS); these results are summarized in Table I. Among small anions, the same permeability sequence was obtained when tested from either side of the membrane: thiocyanate (SCN^-) > NO_3^- > Br^- > Cl^- > I^- > formate ≥ perchlorate (ClO_4^-) > acetate > F^- (Table I). This sequence is similar to the classical lyotropic or Hofmeister series (e.g., Dani et al., 1983), as previously described for unitary CFTR currents (Linsdell et al., 1997*b*; Tabcharani et al., 1997). This suggests that electrodiffusion through CFTR is controlled by a so-called "weak field strength" selectivity site (Wright and Diamond, 1977), with lyotropic (weakly hydrated) anions being preferred over kosmotropic (strongly hydrated) anions (see Collins, 1997).

Asymmetric Permeability of Large Anions

A number of large organic anions yielded surprisingly high apparent permeability ratios, but only when present on the cytoplasmic side of the membrane (Table I; Fig. 1, *C* and *D*). Current was indeed carried by the intracellular anion under these conditions because we found the Na^+ permeability of CFTR to be negligible, and similar permeability ratios were obtained by varying external NaCl or internal Na · anion concentrations. Sodium permeability was measured by replacing 75% of the NaCl in the intracellular solution with sucrose (Fig. 2 *A*). Under these conditions, the current reversal potential shifted by −35.1 ± 0.9 mV (n = 24), which is not significantly different from the value predicted by the Nernst equation for a perfectly Cl^--selective current (−35.4 mV). P_{Na}/P_{Cl} was calculated from the Goldman-Hodgkin-Katz equation:

$$E_{REV} = (RT/F) \ln [(P_{Na}[Na]_o + P_{Cl}[Cl]_i) / (P_{Na}[Na]_i + P_{Cl}[Cl]_o)] \quad (4)$$

where $[X]_o$ and $[X]_i$ refer to extracellular and intracellular ion concentrations, respectively. P_{Na}/P_{Cl} calculated in this way was 0.007 ± 0.010 (n = 24). The apparent permeability of gluconate from the intracellular solution was not significantly altered when intracellular Na^+ was replaced by *N*-methyl-D-glucamine, or when extracellular Na^+ was replaced by Mg^{2+} (data not shown), again suggesting that Na^+ does not contribute significantly to the currents recorded under biionic conditions. The apparent permeability of gluconate from the intracellular solution with 154 mM gluconate in the intracellular solution and 154 mM Cl^- in the extracellular solution ($P_{Gluconate}/P_{Cl}$ = 0.071 ± 0.003, n = 54; see Table I) was similar to that measured when 50% of intracellular Na · gluconate was replaced by sucrose (0.073 ± 0.006; n = 5) or when 70% of extracellular NaCl was replaced by sucrose (0.079 ± 0.02; n = 4), indicating that current was indeed carried by gluconate under these conditions (Fig. 2 *B*).

Examples of the raw current traces from which leak subtracted *I*-V curves such as those illustrated in Figs. 1, *A* and *B*, and 2 were constructed are shown in Fig. 3. All of the raw currents, and the resulting *I*-V curves shown in Fig. 3 were recorded with 154 mM gluconate in the intracellular solution and 154 mM Cl^- in the extracellular solution. Before activation of CFTR, only small leak currents were observed in response to a depolarizing voltage ramp protocol. Activation of CFTR by addition of PKA (in the presence of ATP; Fig. 3 *B*) or ATP (in the presence of PKA; Fig. 3 *C*) stimulated a large increase in current, which was fully reversible on removal of the stimulus. In both cases, the leak-subtracted *I*-V relationship constructed by subtraction of the leak current recorded before stimulation and after wash-out were completely superimposable (Fig. 3, *B* and *C*,

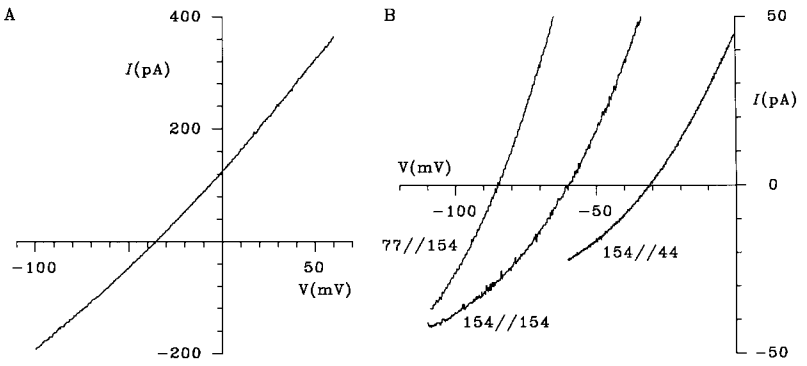

FIGURE 2. Current is carried by intracellular gluconate under biionic conditions. (*A*) Example *I*-V curve when 75% of intracellular NaCl was replaced by sucrose; the reversal potential under these conditions suggests negligible Na^+ permeability (see text). (*B*) The apparent permeability of intracellular gluconate is similar for a range of different ionic conditions. Example *I*-V curves are shown with different concentrations of Na · gluconate in the intracellular solution and NaCl in the extracellular solution, as indicated by $[gluconate]_{in}//[Cl^-]_{out}$. Since the three *I*-V relationships shown in *B* were obtained from different patches, no information is contained in the relative amplitudes of the three curves.

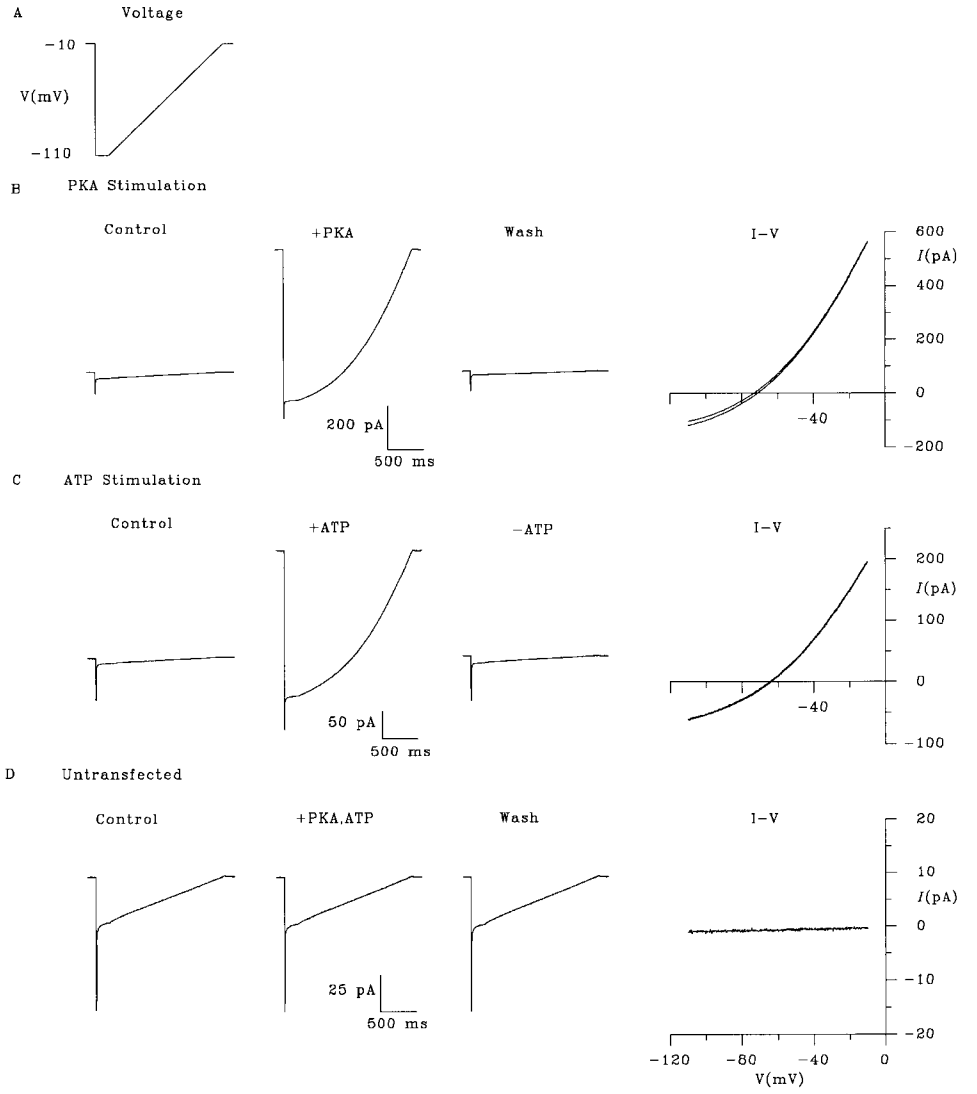

FIGURE 3. Raw current traces illustrating permeation by intracellular gluconate under biionic conditions. (*A*) Voltage ramp protocol used to examine gluconate permeability. (*B*) Current traces recorded in response to the voltage protocol shown in *A*, in the presence of ATP (*Control*), after CFTR stimulation by addition of PKA, and after removal of PKA and ATP (*Wash*). The resulting *I*-*V* curves constructed by subtraction of either of the two leak currents illustrated from the current recorded in the presence of PKA are shown on the right (*I-V*); these two *I*-*V* curves are practically superimposable. (*C*) Current traces recorded in response to the same voltage protocol, in the presence of PKA (*Control*), after CFTR stimulation by addition of ATP, and after removal of ATP. As in *B*, the two resulting indistinguishable *I*-*V* curves are shown at right. (*D*) PKA and ATP do not stimulate any current in patches excised from control, untransfected BHK cells under the conditions used in *B* and *C*.

right), indicating that no change in leak occurred during the course of the experiment. Under these conditions, PKA and ATP did not activate any current in control, untransfected BHK cells (Fig. 3 *D*).

The asymmetry in apparent permeability ratios described in Table I led to large differences in the functional pore diameter estimated under different ionic conditions (Fig. 1, *C* and *D*). Functional pore diameter was estimated from the relationship between ion permeability and unhydrated ionic diameter, as described in METHODS, for each of four sets of conditions: intracellular lyotropic (weakly hydrated; see Collins, 1997) and kosmotropic (strongly hydrated) anions (Fig. 1 *C*) and extracellular lyotropic and kosmotropic anions (Fig. 1 *D*). The fits to Fig. 1, *C* and *D*, suggest a minimum functional pore diameter of 4.9–5.3 Å for intracellular lyotropes and for extracellular lyotropes and kosmotropes, similar to the value we reported previously based on single channel recordings (Linsdell et al., 1997*b*). However, kosmotropic anions with diameters much larger than 5.3 Å were permeant from the cytoplasmic side (Fig. 1 *C*). For these ions, permeability was not strongly dependent on ion size; the fit shown in Fig. 1 *C* suggests a minimum functional pore diameter of 13.8 Å. This discrepancy in functional pore diameter suggests that large organic intracellular anions are handled in an unusual way by CFTR. The structures of the largest anions examined are shown in Fig. 4.

Estimation of Unitary Gluconate Current Amplitude

Gluconate, an example of an anion showing highly asymmetric permeability, does not carry a measurable single channel current through CFTR (Linsdell et al., 1997*b*). However, it is possible to make a rough approximation of the unitary amplitude of the current carried by intracellular gluconate ions from the macroscopic current recorded under biionic conditions (Fig. 5).

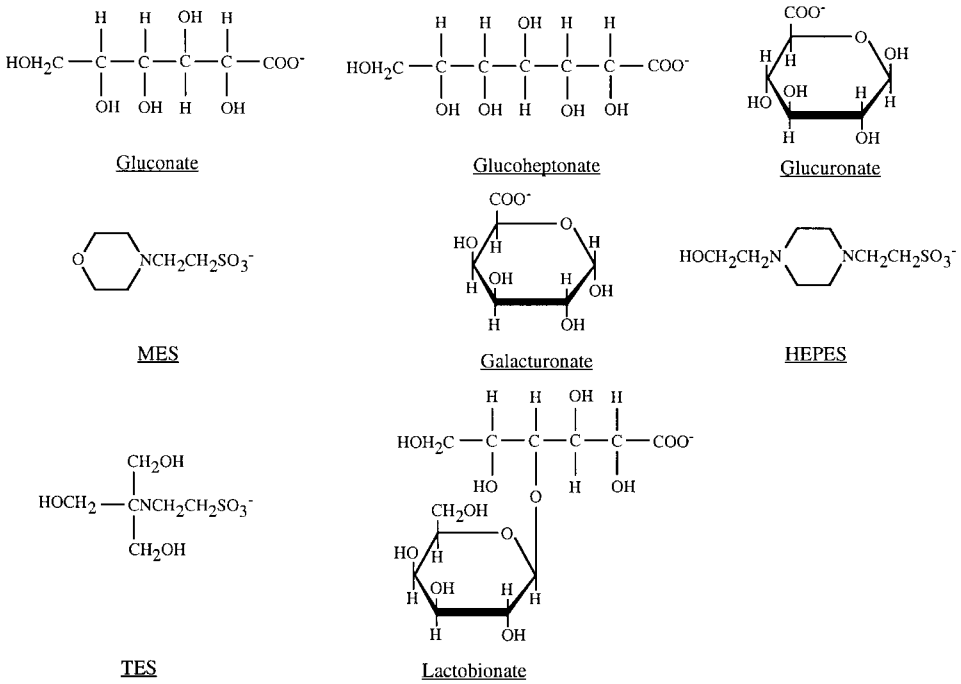

FIGURE 4. Chemical structures of the largest organic anions studied.

With intracellular gluconate, the CFTR Cl^- current measured in excised Chinese hamster ovary cell patches at +50 mV had a unitary amplitude, *i*, of 0.55 ± 0.01 pA (n = 4; Fig. 5 *B*). The macroscopic current amplitude, *I*, at the same potential should be equal to $I = i \cdot n \cdot P_O$, where n is the number of channels in the patch and P_O their mean open probability. P_O cannot be estimated directly from the macroscopic current; however, the polyphosphate pyrophosphate (PPi) causes CFTR to become "locked" in the open state in the presence of ATP (Gunderson and Kopito, 1994; Carson et al., 1995), such that at high PPi concentrations P_O should approach unity. Fig. 5 *D* shows that addition of 10 mM PPi increased both Cl^- influx and gluconate efflux through CFTR without significantly altering the reversal potential. The mean increase in macroscopic Cl^- current amplitude at +50 mV after addition of PPi was 2.15 ± 0.58-fold (n = 15), similar to the mean increase in gluconate current at −100 mV (2.41 ± 0.62-fold, n = 15). The raw current traces used to construct the *I*-V curves shown in Fig. 5 *D* are illustrated in Fig. 5 *E*. As in Fig. 3, *B* and *C*, current returned to its prestimulus level after wash-out of PKA, ATP, and PPi, indicating that no change in leak occurred during the course of the experiment.

Assuming that P_O increases to 1 in the presence of such a high concentration of PPi allows a rough estimate of n from the equation given above; using this method, n was as high as 6,200 channels in one patch. Since P_O may not reach 1 even in the presence of 10 mM PPi, this estimate of n is actually a lower limit. We used our values of n to estimate the unitary gluconate current at −100 mV from the amplitude of the macroscopic current in the presence of PPi at this potential, which gave a unitary current of 40.4 ± 3.3 fA (n = 15). CFTR carries a unitary Cl^- current of 0.77 ± 0.02 pA (n = 3) at this potential with symmetrical 150 mM NaCl solutions.

The unitary gluconate current estimated above, although too small to be resolved using single channel recording, ought to generate significant current noise, which has previously been used to estimate the unitary current amplitude of very low conductance channels (Zweifach and Lewis, 1993; Larsson et al., 1996). Indeed, we found that activation of gluconate current at −50 mV with gluconate present on both sides of the membrane was associated with an increase in current noise (Fig. 6). The relationship between gluconate current amplitude and current variance was described by a parabolic function (Fig. 6), consistent with independent, stochastic gating of ion channels with a single conductance state (Sigworth, 1980; see METHODS). Increasing channel P_O by addition of 1 mM PPi further increased current and decreased current noise (Fig. 6 *B*); under these circumstances, the parabolic relationship between current amplitude and variance was similar to that described in Fig. 6 *A*. At −50 mV with symmetrical gluconate, fitting of variance-vs.-mean current curves such as those shown in Fig. 6, *A* and *B*, with Eq. 3 (see METHODS) gave a unitary gluconate current, *i*, of 38.4 ± 5.5 fA (n = 12), similar to the value estimated above from the macroscopic current amplitude. This suggests a gluconate conductance of 0.77 ± 0.11 pS (n = 12) at this potential.

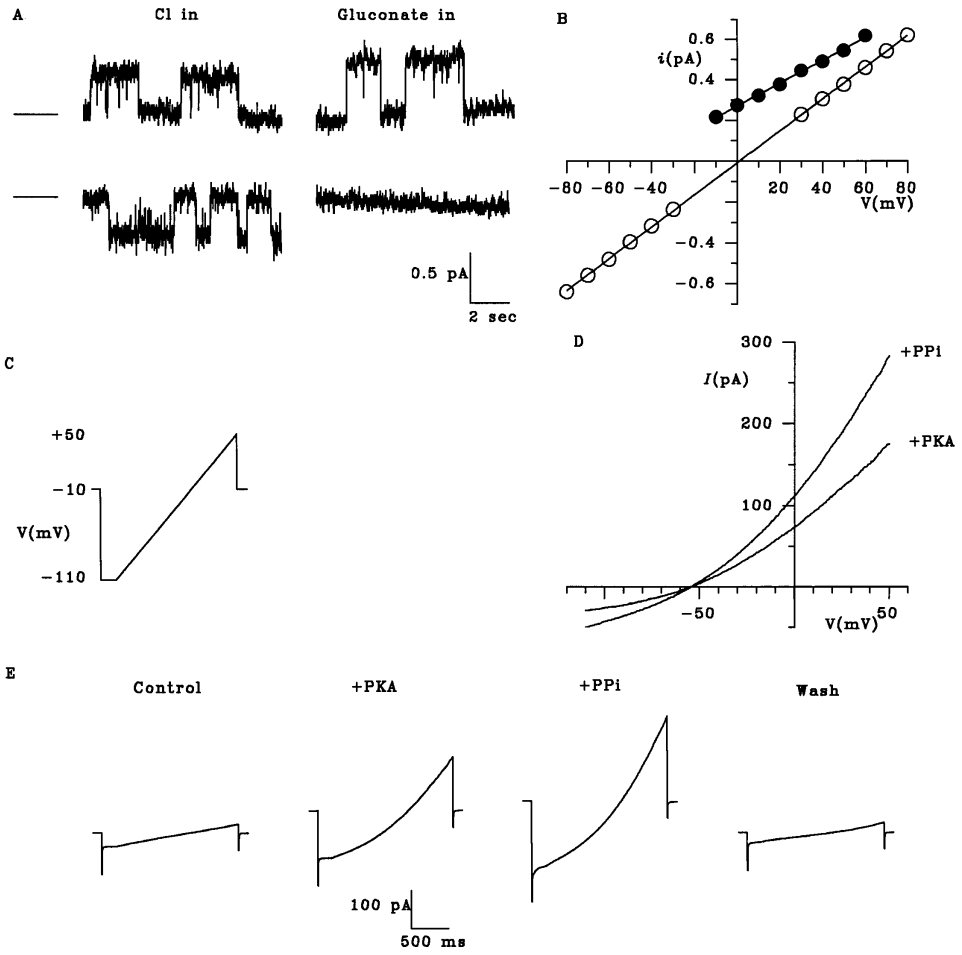

FIGURE 5. Estimation of unitary gluconate current from macroscopic *I*-V curves. (*A*) Unitary CFTR channel currents recorded with 154 mM Cl^- in the extracellular solution and either 154 mM Cl^- (*Cl in*) or 154 mM gluconate (*Gluconate in*) in the intracellular solution, at +50 (*top*) and −50 (*bottom*) mV. In each case, the line on the left represents the closed state of the channel. At negative potentials with gluconate in the intracellular solution, no single channel activity could be resolved. (*B*) Mean single channel *I*-V relationships for CFTR with 154 mM Cl^- in the extracellular solution and 154 mM Cl^- (○) or gluconate (●) in the intracellular solution. Mean of data from 3–18 patches. Unitary Cl^- currents could not be accurately measured with gluconate in the intracellular solution at potentials more negative than −10 mV. (*C*) Voltage ramp protocol used to examine the effects of intracellular PPi on macroscopic Cl^- and gluconate currents. (*D*) Leak-subtracted macroscopic *I*-V relationships showing the effect of intracellular PPi on macroscopic Cl^- and gluconate currents, recorded with intracellular gluconate and external Cl^-. PPi increases current amplitude at all potentials without altering the reversal potential. (*E*) Raw current traces used to construct the *I*-V relationships shown in *D*. Currents were recorded in response to the voltage protocol shown in *C*.

CFTR Mutations Reduce Both Cl^- and Gluconate Conductance

As well as forming a Cl^- channel, CFTR may modulate the activity of a number of other membrane transport proteins (Schwiebert et al., 1995; Stutts et al., 1995; McNicholas et al., 1996). It is possible, therefore, that CFTR could affect the function of an anion transporter endogenous to BHK cells, which could account for the apparent permeability of large organic anions. To determine whether gluconate currents were carried directly via CFTR, we examined gluconate efflux mediated by two low conductance CFTR pore mutants, R347D and K335E (Tabcharani et al., 1993). These mutations in the sixth transmembrane region (TM6) of CFTR both reduce Cl^- conductance by ~50% (Tabcharani et al., 1993). Both R347D (Fig. 7 *A*) and K335E (Fig. 7 *B*) had similar permeabilities to gluconate in the intracellular solution under biionic conditions to that of wild-type CFTR ($P_{Gluconate}/P_{Cl}$ = 0.069 ± 0.010, n = 9, for R347D and 0.064 ± 0.008, n = 7, for K335E), suggesting that relative permeability to large organic anions from the intracellular solution is not disrupted in either of these mutants. This is consistent with our previous finding that selectivity among smaller anions is not altered in either of these mutants (Linsdell, P., and J.W. Hanrahan, unpublished observations). For both mutants, activation of gluconate current under symmetrical ionic conditions was associated with a significantly smaller increase in current noise than was seen for wild type (Fig. 7, *C* and *D*). Fitting the relationship between macroscopic gluconate current amplitude at −50 mV and current variance (Fig. 7, *C* and *D*) gave unitary gluconate current amplitudes of 13.4 ±

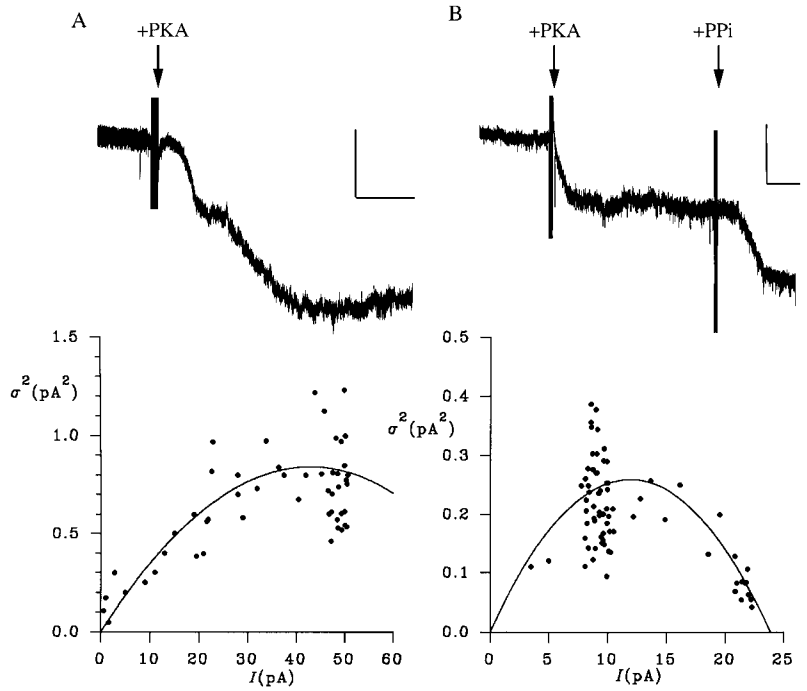

FIGURE 6. Estimation of unitary gluconate current from macroscopic gluconate current noise. (*A*) Slow activation of gluconate current at −50 mV under symmetrical ionic conditions on addition of PKA. The scale bar represents 10 pA and 1 min. Below is shown the relationship between mean gluconate current (I) and current variance (σ^2) for this patch, calculated for 5-s subrecords as described in METHODS. The data have been fitted by Eq. 3 (see METHODS), giving i = 39.3 fA and n = 2,183. (*B*) Macroscopic gluconate current under these conditions is further stimulated by addition of 1 mM PPi, and this increase in current is associated with a decrease in current variance. The relationship between I and σ^2 for this patch has been fitted by Eq. 3 (see METHODS), giving i = 43.4 fA and n = 549.

3.9 fA (n = 3) for R347D and 18.1 ± 3.4 fA (n = 5) for K335E, in both cases significantly smaller than wild type under these conditions ($P < 0.05$, two-tailed t test). The fact that unitary gluconate current amplitude is reduced by mutations within the pore region of CFTR is strong evidence that gluconate efflux occurs directly via the CFTR molecule. Furthermore, the fact that these mutations cause similar reductions in channel conductance to both Cl^- and gluconate suggests that Cl^- and gluconate share a common permeation pathway through CFTR.

Block of Cl^- and Gluconate Currents

Further evidence that gluconate and Cl^- share a common permeation pathway is their similar sensitivity to

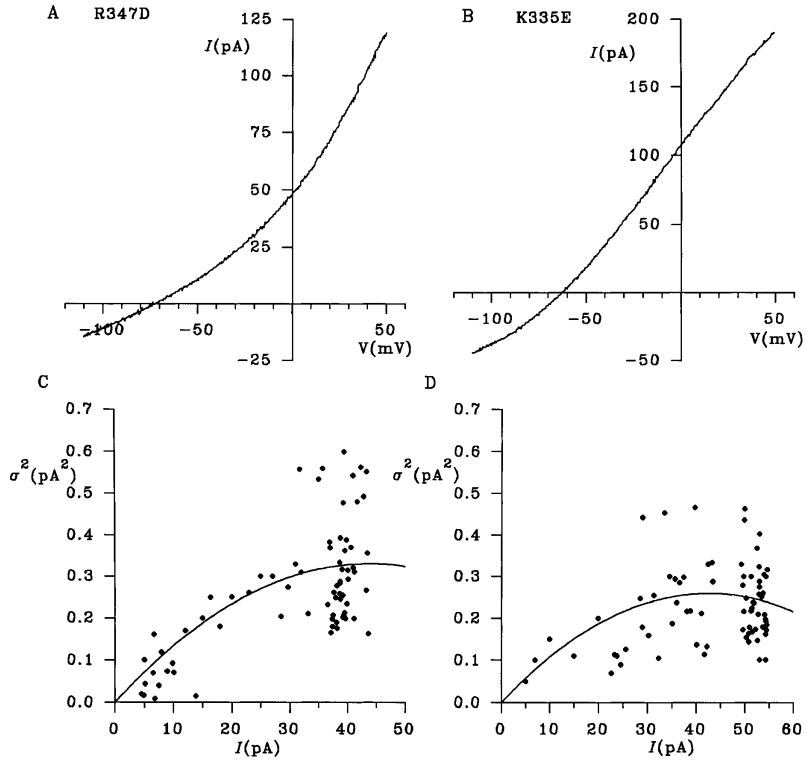

FIGURE 7. Gluconate conductance of CFTR pore mutants. Both R347D (*A*) and K335E (*B*) mediate macroscopic gluconate efflux with a similar apparent gluconate permeability to wild type (see Figs. 1 *A*, 2 *B*, 3, *B* and *C*, 5 *D*, and 8, *A* and *B*). (*C* and *D*) Relationship between mean gluconate current (I) and current variance (σ^2) at −50 mV under symmetrical ionic conditions for R347D (*C*) and K335E (*D*), calculated as described in Fig. 6 *A*. In each case, the data have been fitted by Eq. 3 (see METHODS), giving i = 15.1 fA and n = 5,795 in *C*, and i = 12.1 fA and n = 6,967 in *D*.

open channel blockers (Fig. 8). Cl^- permeation through CFTR is blocked by intracellular 4,4′-dinitrostilbene-2,2′-disulfonic acid (Linsdell and Hanrahan, 1996*a*) and glibenclamide (Sheppard and Welsh, 1992; Schultz et al., 1996; Sheppard and Robinson, 1997). Both of these substances appear to act as open channel blockers of CFTR; DNDS has been shown to interact with a known pore-lining amino acid (R347; Linsdell and Hanrahan, 1996*a*), and block by intracellular glibenclamide is sensitive to the extracellular Cl^- concentration (Sheppard and Robinson, 1997; Linsdell and Hanrahan, 1997), a hallmark of an open-channel block mechanism. The location of the glibenclamide binding site on CFTR is unknown; it does not seem to involve R347 (Linsdell and Hanrahan, 1997). We found that both DNDS (200 μM; Fig. 8 *A*) and glibenclamide (60 μM; Fig. 8 *B*) blocked gluconate efflux under biionic conditions when added to the intracellular solution. At these concentrations, the amplitude of the gluconate current at −100 mV was reduced to 16.7 ± 3.9% of its control value by DNDS (n = 7) and to 17.4 ± 4.8% of control

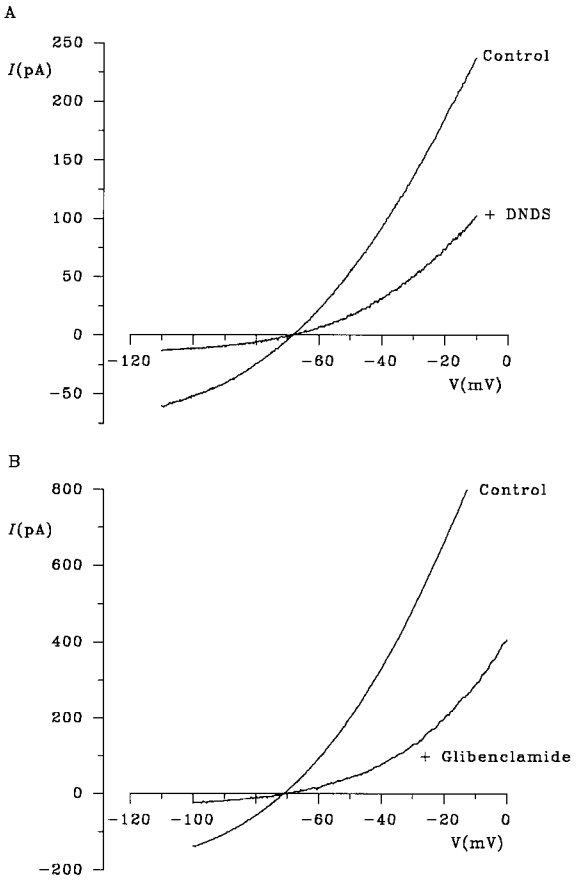

FIGURE 8. Blocker sensitivity of gluconate efflux. Examples of macroscopic *I*-*V* relationships recorded under biionic conditions (internal gluconate, external Cl^-) before (*Control*) and immediately after addition of 200 μM DNDS (*A*) or 60 μM glibenclamide (*B*) are shown. Both DNDS and glibenclamide block gluconate efflux and Cl^- influx in a voltage-dependent manner.

by glibenclamide (n = 5), effects similar to the block of CFTR Cl^- current at this potential (Linsdell and Hanrahan, 1996*a*, 1997; Sheppard and Robinson, 1997). That these blockers have similar effects on gluconate and Cl^- permeation is supported by the fact that block is not associated with a change in the current reversal potential under biionic conditions (Fig. 8). Block by DNDS and glibenclamide provides further evidence that gluconate efflux occurs directly via CFTR, and that gluconate and Cl^- share a common permeation pathway.

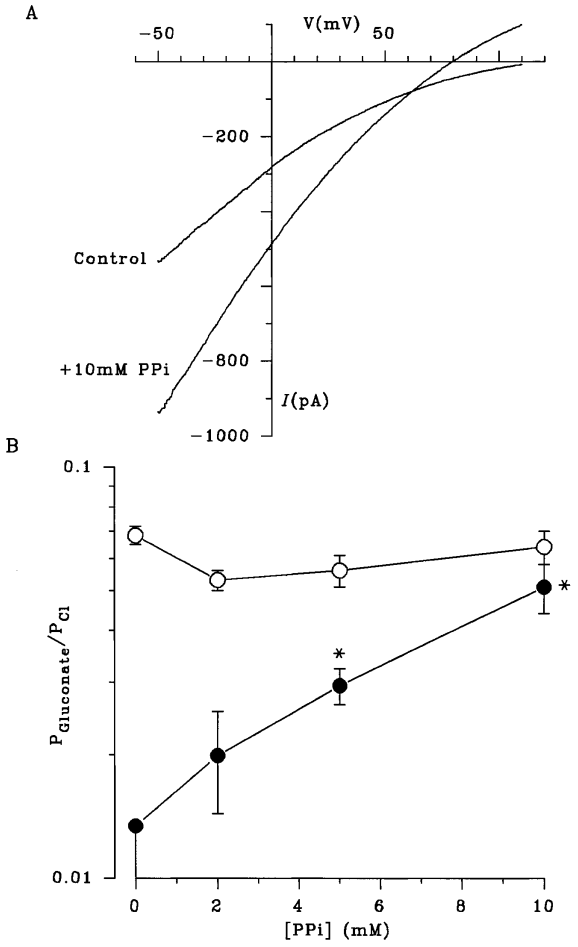

FIGURE 9. PPi disrupts the asymmetry of gluconate permeability by allowing gluconate influx from the extracellular solution. (*A*) PPi allows the influx of the normally impermeant gluconate from the extracellular solution under biionic conditions. The increase in extracellular gluconate permeability caused by PPi is seen more clearly in *B*, which shows mean gluconate permeability ($P_{Gluconate}/P_{Cl}$) as a function of PPi concentration, when gluconate is present in the internal (○) or external (●) solution. Each point represents the mean of data from 36 patches in the absence of PPi, and 3–9 patches at different PPi concentrations. The value of $P_{Gluconate}/P_{Cl}$ for external gluconate in the absence of PPi (0.013) is a maximum value since no reversal was observed under these conditions (n = 36). The actual value for $P_{Gluconate}/P_{Cl}$ under these conditions is likely to be considerably lower; it may be zero. In contrast, a clear current reversal was observed with external gluconate in 13 of 13 patches in the presence of 2–10 mM PPi. *$P_{Gluconate}/P_{Cl}$ is significantly greater than 0.013 ($P < 0.01$, one-tailed t test).

Asymmetric Large Anion Permeability Requires ATP Hydrolysis

Both Cl^- influx and gluconate efflux under biionic conditions were increased in the presence of the ATPase inhibitor PPi (Fig. 5 *D*), presumably due to locking of channels in the open state (Gunderson and Kopito, 1994; Carson et al., 1995). The increase in gluconate current caused by PPi was not associated with any change in apparent gluconate permeability from the intracellular solution (Figs. 5 *D* and 9 *B*). In contrast, when gluconate was present in the extracellular solution under biionic conditions, PPi caused a concentration-dependent stimulation of gluconate influx, leading to a measurable apparent permeability for gluconate from the extracellular solution (Fig. 9). At the highest concentration of PPi used (10 mM), gluconate showed a similar permeability from the extracellular and intracellular solutions (Fig. 9 *B*). Similar effects were observed when the larger organic anions, glucuronate, galacturonate, or lactobionate, were present in the extracellular solution under biionic conditions (Fig. 10). These effects of PPi strongly suggest that ATP hydrolysis is required to maintain the asymmetrical nature of permeation by large organic anions.

As described above, PPi locks CFTR channels in a conducting open state, which has been interpreted as a requirement for ATP hydrolysis to close the channel (Gunderson and Kopito, 1994; Carson et al., 1995). This effect is shared by nonhydrolyzable ATP analogues such as 5′-adenylylimidodiphosphate (AMP-PNP; Hwang et al., 1994). As shown in Fig. 11, AMP-PNP also stimulated significant gluconate influx through CFTR under biionic conditions. In contrast, another ATPase inhibitor, sodium azide (NaN_3), which inhibits CFTR channel opening (Li et al., 1996*b*; Fig. 11) did not allow gluconate influx, suggesting a link between channel locking in the open state and disruption of the asymmetry in gluconate permeability. ADP also inhibits CFTR, presumably by competing with ATP (Anderson and Welsh, 1992); we found that ADP also inhibited CFTR Cl^- current without allowing gluconate influx (Fig. 11).

DISCUSSION

The biionic permeability of CFTR to small anions is similar to a number of other Cl^- channels, showing lyotropic anion selectivity and a functional minimum pore diameter of ~5.3 Å (Fig. 1; Table I). However, the channel also shows anomalous permeability to a wide range of large organic anions when these ions are present in the intracellular (but not extracellular) solution. This asymmetry in large anion permeability appeared to be linked to ATP hydrolysis by CFTR, since it was abolished by the ATPase inhibitors PPi and AMP-PNP (Figs. 9–11).

It has previously been suggested that CFTR may allow the rapid electrodiffusion of ATP (Reisin et al., 1994; Schwiebert et al., 1995), although this has been disputed by some (Grygorczyk et al., 1996; Li et al., 1996*a*; Reddy et al., 1996). We found that anion efflux was not observed with all intracellular anions (e.g., PF_6; Fig. 1,

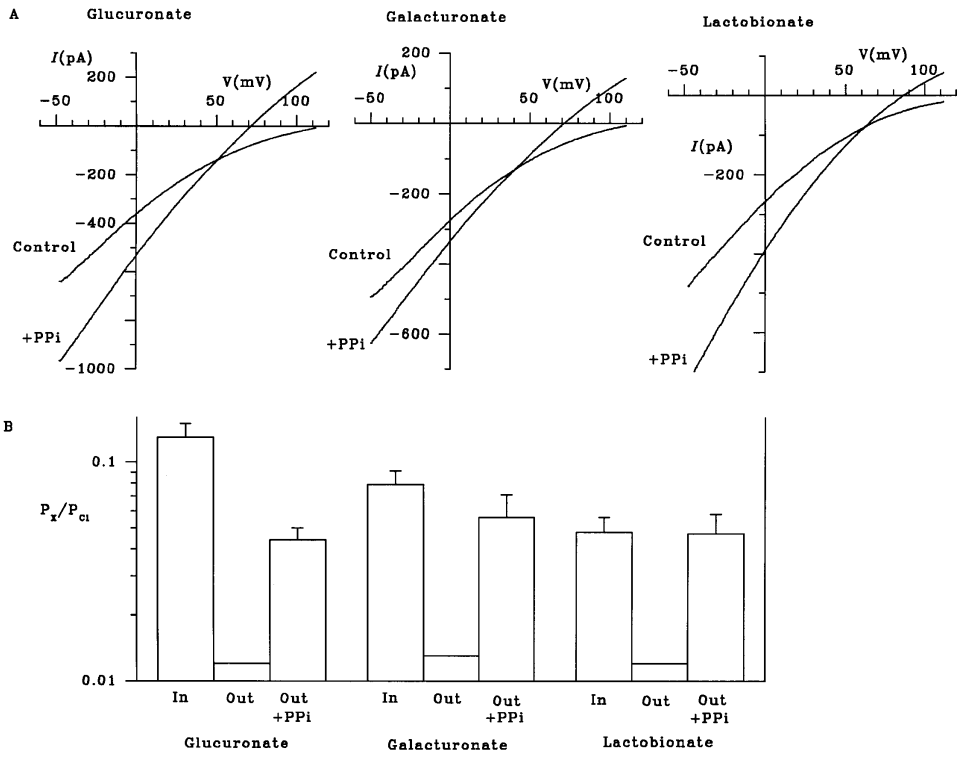

FIGURE 10. PPi stimulates influx of a number of large organic anions from the extracellular solution. (*A*) Addition of 10 mM PPi allows the influx of the normally impermeant anions glucuronate, galacturonate, and lactobionate from the extracellular solution under biionic conditions. (*B*) Mean permeability of each of these anions when they are present in the intracellular (*In*) or extracellular (*Out*) solution under biionic conditions. In each case, the values of P_X/P_{Cl} for large anions in the extracellular solution in the absence of PPi are maximum values (see Fig. 9 *B*). Mean of data from four to five patches. In each case, addition of PPi increased the permeability of the extracellular anion to a value significantly greater than the maximum permeability shown in the absence of PPi ($P < 0.05$, one-tailed *t* test).

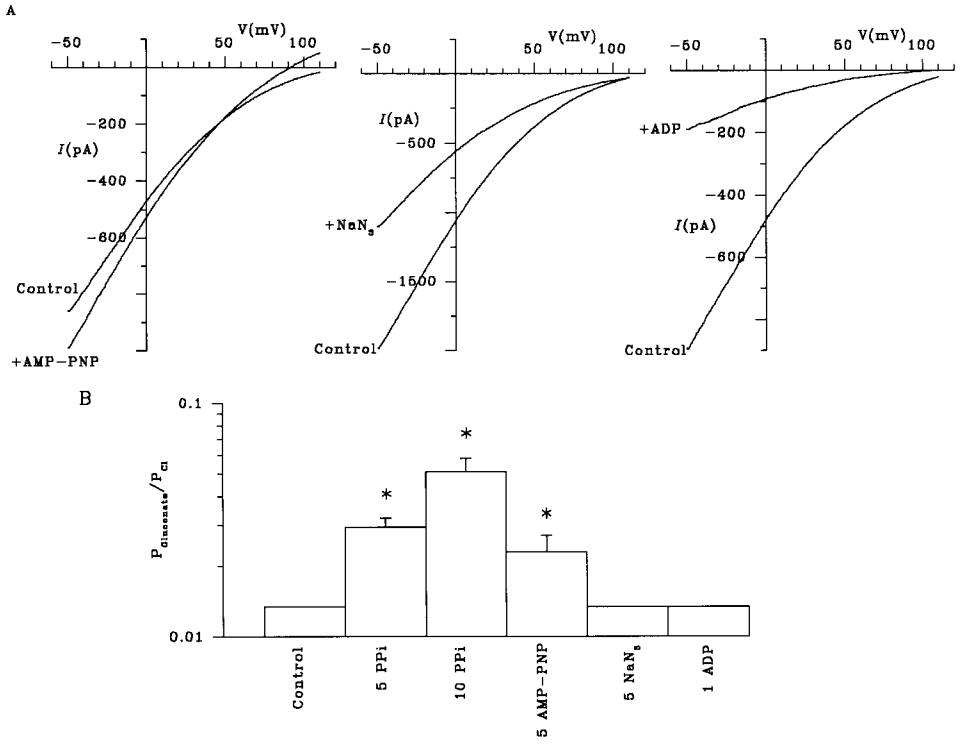

FIGURE 11. Different ATPase inhibitors differentially affect external gluconate permeability. (*A*) AMP-PNP (5 mM) has a similar effect to PPi (Fig. 9 *A*), increasing Cl^- efflux and stimulating gluconate influx. In contrast, both NaN_3 (5 mM) and ADP (1 mM) reduced Cl^- efflux without allowing any measurable gluconate influx. (*B*) Mean values of $P_{Gluconate}/P_{Cl}$ for gluconate in the extracellular solution under different conditions. The values for NaN_3 and ADP, like those for control, are maximum values (see Fig. 9 *B*). Mean of data from 36 patches for control and 4–5 patches under other conditions. $*P_{Gluconate}/P_{Cl}$ is significantly greater than 0.013 ($P < 0.05$, one-tailed *t* test; see Fig. 9 *B*).

A and *C*), even in the presence of intracellular ATP. Furthermore, positive currents (carried by anion influx) were induced by the ATPase inhibitors PPi and AMP-PNP in the absence of extracellular ATP (Figs. 9–11). Both these findings strongly suggest that ATP transport did not contribute to measured anion currents in our experiments. Nevertheless, the finding that the permeation properties of CFTR can be strongly affected by alterations in ATPase activity do not exclude the possibility that ATP permeation may occur under certain conditions.

In addition to forming a Cl^- channel, CFTR may also modulate the activity of other membrane transport proteins (Schwiebert et al., 1995; Stutts et al., 1995; McNicholas et al., 1996). However, anion export in BHK cell patches was due to CFTR itself and not the result of modification of an anion transporter endogenous to these cells, since the apparent unitary gluconate current amplitude was significantly reduced in two CFTR mutants with reduced Cl^- conductance, R347D and K335E (Fig. 7). The similar pharmacology of Cl^- and gluconate currents carried by CFTR further suggests that these ions share a common permeation pathway (Fig. 8). Although neither DNDS nor glibenclamide are specific blockers of CFTR, the similarity of their effects on Cl^- and gluconate permeation supports the hypothesis that CFTR itself carries both Cl^- and gluconate currents.

A unique property of large anion permeation through the CFTR channel was its strong asymmetry. All organic anions tested were permeant when present in the intracellular solution under biionic conditions, with relative permeabilities (P_X/P_{Cl}) in the range 0.048–0.25 (Fig. 1 *C*; Table I). In contrast, only the smallest organic anions tested (formate, acetate, propanoate) were measurably permeant when present in the extracellular solution under biionic conditions. Weak asymmetry in ionic permeability depending on the orientation of the ionic species relative to the membrane has previously been observed in both potassium channels (Wagoner and Oxford, 1987; Heginbotham and MacKinnon, 1993; Pérez-Cornejo and Begenisich, 1994; Reuveny et al., 1996) and sodium channels (Garber, 1988), where it has been taken as evidence that these channels have multi-ion pores (see below). However, in all these cases, asymmetric permeability occurred for ions that were quite permeant when present on either side of the membrane; we are unaware of any previous examples of channels that are apparently permeable to some ions from one side of the membrane but not the other.

The asymmetric ionic permeabilities observed, although extreme, could still be consistent with permeation in a highly asymmetric, multi-ion pore. A functional asymmetry in the ability of large organic anions to enter the CFTR pore is also implied by our previous finding that intracellular, but not extracellular, gluconate ions can block Cl^- permeation through the open channel (Linsdell and Hanrahan, 1996*b*). We have also demonstrated that ion permeation in CFTR reveals several characteristics of a multi-ion pore (Tabcharani et

al., 1993; Linsdell et al., 1997*a*). However, it is intriguing that the ATPase inhibitors PPi and AMP-PNP (but not NaN_3 or ADP) allow gluconate influx from the extracellular solution (Figs. 9 and 11); this indicates that the asymmetry itself requires ATP hydrolysis. At the highest concentration of PPi used, gluconate permeability was similar whether it was present in the intracellular or extracellular solution (Fig. 9 *B*). PPi also stimulated the influx of the other large anions, glucuronate, galacturonate, and lactobionate (Fig. 10). The fact that gluconate influx can be stimulated by ATPase inhibitors that lock CFTR channels in the open state (PPi, AMP-PNP) but not those that reduce channel open probability (NaN_3, ADP) suggests that there may be a link between channel gating and permeability to large organic anions. It has previously been suggested that ATP hydrolysis by CFTR may be required for an irreversible gating step between two distinct open states with different functional pore properties (Gunderson and Kopito, 1995; Ishihara and Welsh, 1997).

The functional minimum pore diameter suggested by the permeability of all extracellular anions, as well as intracellular lyotropes (~5.3 Å; Fig. 1, *C* and *D*) is similar to what we calculated previously from single channel experiments (Linsdell et al., 1997*b*). However, the pore is clearly capable of adopting a much larger conformation to allow anions as large as lactobionate (unhydrated dimensions 7.57 × 9.32 × 13.11 Å; Table I) to permeate at a low rate. These results emphasize that the pore diameter estimated using the "excluded volume effect" method of Fig. 1, *C* and *D*, is a functional rather than structural parameter. Nevertheless, the reappraisal of the physical dimensions of the pore suggested by our present results has important implications for the structure of CFTR. The structurally related ABC protein P-glycoprotein has been suggested, based on electron microscopy, to have a central aqueous pore of ~50 Å in diameter (Rosenberg et al., 1997).

Numerous other Cl^- channels have been suggested to have minimum functional pore diameters similar to what we estimated from the permeability of lyotropic anions in Fig. 1, *C* and *D* (5.2–6.4 Å; Bormann et al., 1987; Franciolini and Nonner, 1987; Halm and Frizzell, 1992; Fatima-Shad and Barry, 1993; Arreola et al., 1995). Of course, as described above, these functional diameters should not be used to assign physical dimensions to ion channel pores (see Finkelstein, 1987). A number of anion-selective channels, especially those proposed to play a role in cell volume regulation, show considerable permeability both to organic anions and uncharged organic osmolytes (for recent reviews, see Strange and Jackson, 1995; Kirk, 1997; Okada, 1997). The symmetry of permeation in such channels has not been examined.

The ability of a broad range of large organic anions to permeate through CFTR from the intracellular solution has important implications both for the role of CFTR in normal epithelial cells and for the functional consequences of its absence in cystic fibrosis. The ability to pass large cytoplasmic organic anions is also reminiscent of the closely related ABC proteins multidrug resistance protein (MRP; Cole et al., 1992) and canalicular multispecific organic anion transporter (cMOAT; also known as MRP2; Paulusma et al., 1996), both of which mediate the ATP-dependent transport of a wide range of large organic anions across the membrane from the intracellular side. The ability to mediate the efflux of a broad range of large organic anions from the cytoplasm may therefore be a common function of all these ABC proteins, whether or not transport is achieved by exactly the same mechanism. Interestingly, it has recently been proposed that MRP may be able to functionally substitute for CFTR in human airways, and that MRP overexpression (for example, as a result of cancer chemotherapy) may be of therapeutic use in cystic fibrosis (Lallemand et al., 1997). It was suggested that MRP may complement "a still undescribed CFTR function" (Lallemand et al., 1997). We propose that one such function of CFTR may be to mediate the efflux of large organic anions.

We thank Shu-Xian Zheng and Jie Liao for technical assistance and Dr. J.M. Rommens (Hospital for Sick Children, Toronto, Ontario, Canada) for providing R347D and K335E cDNA.

This work was supported by the Canadian Cystic Fibrosis Foundation (CCFF), Canadian Medical Research Council (MRC), and the National Institute of Diabetes and Digestive and Kidney Diseases. P. Linsdell is a CCFF postdoctoral fellow and J.W. Hanrahan is an MRC scientist.

Original version received 25 September 1997 and accepted version received 10 February 1998.

REFERENCES

Anderson, M.P., and M.J. Welsh. 1992. Regulation by ATP and ADP of CFTR chloride channels that contain mutant nucleotide-binding domains. *Science.* 257:1701–1704.

Arreola, J., J.E. Melvin, and T. Begenisich. 1995. Volume-activated chloride channels in rat parotid acinar cells. *J. Physiol. (Camb.).* 484:677–687.

Bormann, J., O.P. Hamill, and B. Sakmann. 1987. Mechanism of anion permeation through channels gated by glycine and γ-aminobutyric acid in mouse cultured spinal neurones. *J. Physiol. (Camb.).* 385:243–286.

Carson, M.R., M.C. Winter, S.M. Travis, and M.J. Welsh. 1995. Pyrophosphate stimulates wild-type and mutant cystic fibrosis transmembrane conductance regulator Cl^- channels. *J. Biol. Chem.* 270:20466–20472.

Cole, S.P.C., G. Bhardwaj, J.H. Gerlach, J.E. Mackie, C.E. Grant, K.C. Almquist, A.J. Stewart, E.U. Kurz, A.M.V. Duncan, and R.G. Deeley. 1992. Overexpression of a transporter gene in a multidrug-resistant human lung cancer cell line. *Science.* 258:1650–1654.

Collins, K.D. 1997. Charge density-dependent strength of hydration and biological structure. *Biophys. J.* 72:65–76.

Dani, J.A., J.A. Sanchez, and B. Hille. 1983. Lyotropic anions. Na channel gating and Ca electrode response. *J. Gen. Physiol.* 81:255–281.

Dwyer, T.M., D.J. Adams, and B. Hille. 1980. The permeability of the endplate channel to organic cations in frog muscle. *J. Gen. Physiol.* 75:469–492.

Fatima-Shad, K., and P.H. Barry. 1993. Anion permeation in GABA- and glycine-gated channels of mammalian cultured hippocampal neurons. *Proc. R. Soc. Lond. B Biol. Sci.* 253:69–75.

Finkelstein, A. 1987. Water Movement Through Lipid Bilayers, Pores, and Plasma Membranes. Theory and Reality. John Wiley & Sons, New York. 228 pp.

Franciolini, F., and W. Nonner. 1987. Anion and cation permeability of a chloride channel in rat hippocampal neurons. *J. Gen. Physiol.* 90:453–478.

Gadsby, D.C., G. Nagel, and T.-C. Hwang. 1995. The CFTR chloride channel of mammalian heart. *Annu. Rev. Physiol.* 57:387–416.

Garber, S.S. 1988. Symmetry and asymmetry of permeation through toxin-modified Na^+ channels. *Biophys. J.* 54:767–776.

Grygorczyk, R., J.A. Tabcharani, and J.W. Hanrahan. 1996. CFTR channels expressed in CHO cells do not have detectable ATP conductance. *J. Membr. Biol.* 151:139–148.

Gunderson, K.L., and R.R. Kopito. 1994. Effects of pyrophosphate and nucleotide analogs suggest a role for ATP hydrolysis in cystic fibrosis transmembrane regulator channel gating. *J. Biol. Chem.* 269:19349–19353.

Gunderson, K.L., and R.R. Kopito. 1995. Conformational states of CFTR associated with channel gating: the role of ATP binding and hydrolysis. *Cell.* 82:231–239.

Halm, D.R., and R.A. Frizzell. 1992. Anion permeation in an apical membrane chloride channel of a secretory epithelial cell. *J. Gen. Physiol.* 99:339–366.

Hanrahan, J.W., J.A. Tabcharani, F. Becq, C.J. Mathews, O. Augustinas, T.J. Jensen, X.-B. Chang, and J.R. Riordan. 1995. Function and dysfunction of the CFTR chloride channel. *In* Ion Channels and Genetic Diseases. D.C. Dawson and R.A. Frizzell, editors. The Rockefeller University Press, New York. 125–137.

Heginbotham, L., and R. MacKinnon. 1993. Conduction properties of the cloned *Shaker* K^+ channel. *Biophys. J.* 65:2089–2096.

Higgins, C.F. 1995. The ABC of channel regulation. *Cell.* 82:693–696.

Hwang, T.-C., G. Nagel, A.C. Nairn, and D.C. Gadsby. 1994. Regulation of the gating of cystic fibrosis transmembrane conductance regulator Cl channels by phosphorylation and ATP hydrolysis. *Proc. Natl. Acad. Sci. USA.* 91:4698–4702.

Ishihara, H., and M.J. Welsh. 1997. Block by MOPS reveals a conformation change in the CFTR pore produced by ATP hydrolysis. *Am. J. Physiol.* 273:C1278–C1289.

Kirk, K. 1997. Swelling-activated organic osmolyte channels. *J. Membr. Biol.* 158:1–16.

Lallemand, J.Y., V. Stoven, J.P. Annereau, J. Boucher, S. Blanquet, J. Barthe, and G. Lenoir. 1997. Induction by antitumoral drugs of proteins that functionally complement CFTR: a novel therapy for cystic fibrosis? *Lancet.* 350:711–712.

Larsson, H.P., S.A. Picaud, F.S. Werblin, and H. Lecar. 1996. Noise analysis of the glutamate-activated current in photoreceptors. *Biophys. J.* 70:733–742.

Li, C., M. Ramjeesingh, and C.E. Bear. 1996*a*. Purified cystic fibrosis transmembrane conductance regulator (CFTR) does not function as an ATP channel. *J. Biol. Chem.* 271:11623–11626.

Li, C., M. Ramjeesingh, W. Wang, E. Garami, M. Hewryk, D. Lee, J.M. Rommens, K. Galley, and C.E. Bear. 1996*b*. ATPase activity of the cystic fibrosis transmembrane conductance regulator. *J. Biol. Chem.* 271:28463–28468.

Linsdell, P., and J.W. Hanrahan. 1996*a*. Disulphonic stilbene block of cystic fibrosis transmembrane conductance regulator Cl^- channels expressed in a mammalian cell line and its regulation by a critical pore residue. *J. Physiol. (Camb.).* 496:687–693.

Linsdell, P., and J.W. Hanrahan. 1996*b*. Flickery block of single CFTR chloride channels by intracellular anions and osmolytes. *Am. J. Physiol.* 271:C628–C634.

Linsdell, P., and J.W. Hanrahan. 1997. Interaction of channel blockers with R347D-CFTR. *Pediatr. Pulm. Suppl.* 14:215. (Abstr.)

Linsdell, P., J.A. Tabcharani, and J.W. Hanrahan. 1997*a*. Multi-ion mechanism for ion permeation and block in the cystic fibrosis transmembrane conductance regulator chloride channel. *J. Gen. Physiol.* 110:365–377.

Linsdell, P., J.A. Tabcharani, J.M. Rommens, Y.-X. Hou, X.-B. Chang, L.-C. Tsui, J.R. Riordan, and J.W. Hanrahan. 1997*b*. Permeability of wild-type and mutant cystic fibrosis transmembrane conductance regulator chloride channels to polyatomic anions. *J. Gen. Physiol.* 110:355–364.

McNicholas, C.M., W.B. Guggino, E.M. Schwiebert, S.C. Hebert, G. Giebisch, and M.E. Egan. 1996. Sensitivity of a renal K^+ channel (ROMK2) to the inhibitory sulfonylurea compound glibenclamide is enhanced by coexpression with the ATP-binding cassette transporter cystic fibrosis transmembrane conductance regulator. *Proc. Natl. Acad. Sci. USA.* 93:8083–8088.

Okada, Y. 1997. Volume expansion-sensing outward-rectifier Cl^- channel: fresh start to the molecular identity and volume sensor. *Am. J. Physiol.* 273:C755–C789.

Paulusma, C.C., P.J. Bosma, G.J.R. Zaman, C.T.M. Bakker, M. Otter, G.L. Scheffer, R.J. Scheper, P. Borst, and R.P.J. Oude Elferink. 1996. Congenital jaundice in rats with a mutation in a multidrug resistance-associated protein gene. *Science.* 271:1126–1128.

Pérez-Cornejo, P., and T. Begenisich. 1994. The multi-ion nature of the pore in *Shaker* K^+ channels. *Biophys. J.* 66:1929–1938.

Reddy, M.M., P.M. Quinton, C. Haws, J.J. Wine, R. Grygorczyk, J.A. Tabcharani, J.W. Hanrahan, K.L. Gunderson, and R.R. Kopito. 1996. Failure of the cystic fibrosis transmembrane conductance regulator to conduct ATP. *Science.* 271:1876–1879.

Reisin, I.L., A.G. Prat, E.H. Abraham, J.F. Amara, R.J. Gregory, D.A. Ausiello, and H.F. Cantiello. 1994. The cystic fibrosis transmembrane conductance regulator is a dual ATP and chloride channel. *J. Biol. Chem.* 269:20584–20591.

Reuveny, E., Y.N. Jan, and L.Y. Jan. 1996. Contributions of a negatively charged residue in the hydrophobic domain of the IRK1 inwardly rectifying K^+ channel to K^+-selective permeation. *Biophys. J.* 70:754–761.

Riordan, J.R., J.M. Rommens, B. Kerem, A. Alon, R. Rozmahel, Z. Grzelczak, J. Zielenski, S. Lok, N. Plasvik, J.-L. Chou, et al. 1989. Identification of the cystic fibrosis gene: cloning and characterization of complementary DNA. *Science.* 245:1066–1073.

Rosenberg, M.F., R. Callaghan, R.C. Ford, and C.F. Higgins. 1997. Structure of the multidrug resistance P-glycoprotein to 2.5nm resolution determined by electron microscopy and image analysis. *J. Biol. Chem.* 272:10685–10694.

Schultz, B.D., A.D.G. DeRoos, C.J. Venglarik, A.K. Singh, R.A. Frizzell, and R.J. Bridges. 1996. Glibenclamide blockade of CFTR chloride channels. *Am. J. Physiol.* 271:L192–L200.

Schwiebert, E.M., M.E. Egan, T.-H. Hwang, S.B. Fulmer, S.S. Allen,

G.R. Cutting, and W.B. Guggino. 1995. CFTR regulates outwardly rectifying chloride channels through an autocrine mechanism involving ATP. *Cell.* 81:1063–1073.

Seibert, F.S., J.A. Tabcharani, X.-B. Chang, A.M. Dulhanty, C. Mathews, J.W. Hanrahan, and J.R. Riordan. 1995. cAMP-dependent protein kinase-mediated phosphorylation of cystic fibrosis transmembrane conductance regulator residue Ser-753 and its role in channel activation. *J. Biol. Chem.* 270:2158–2162.

Sheppard, D.N., and K.A. Robinson. 1997. Mechanism of glibenclamide inhibition of cystic fibrosis transmembrane conductance regulator Cl^- channels expressed in a murine cell line. *J. Physiol. (Camb.).* 503:333–346.

Sheppard, D.N., and M.J. Welsh. 1992. Effect of ATP-sensitive K^+ channel regulators on cystic fibrosis transmembrane conductance regulator chloride currents. *J. Gen. Physiol.* 100:573–591.

Sigworth, F.J. 1980. The variance of sodium current fluctuations at the node of Ranvier. *J. Physiol. (Camb.).* 307:97–129.

Strange, K., and P.S. Jackson. 1995. Swelling-activated organic osmolyte efflux: a new role for anion channels. *Kidney Int.* 48:994–1003.

Stutts, M.J., C.M. Canessa, J.C. Olsen, M. Hamrick, J.A. Cohn, B.C. Rossier, and R.C. Boucher. 1995. CFTR as a cAMP-dependent regulator of sodium channels. *Science.* 269:847–850.

Tabcharani, J.A., X.-B. Chang, J.R. Riordan, and J.W. Hanrahan. 1991. Phosphorylation-regulated Cl^- channel in CHO cells stably expressing the cystic fibrosis gene. *Nature.* 352:628–631.

Tabcharani, J.A., P. Linsdell, and J.W. Hanrahan. 1997. Halide permeation in wild-type and mutant cystic fibrosis transmembrane conductance regulator chloride channels. *J. Gen. Physiol.* 110:341–354.

Tabcharani, J.A., J.M. Rommens, Y.-X. Hou, X.-B. Chang, L.-C. Tsui, J.R. Riordan, and J.W. Hanrahan. 1993. Multi-ion pore behaviour in the CFTR chloride channel. *Nature.* 366:79–82.

Tusnády, G.E., E. Bakos, A. Váradi, and B. Sarkadi. 1997. Membrane topology distinguishes a subfamily of the ATP-binding cassette (ABC) transporters. *FEBS Lett.* 402:1–3.

Wagoner, P.K., and G.S. Oxford. 1987. Cation permeation through the voltage-dependent potassium channel in the squid axon. Characteristics and mechanisms. *J. Gen. Physiol.* 90:261–290.

Wright, E.M., and J.M. Diamond. 1977. Anion selectivity in biological systems. *Physiol. Rev.* 57:109–156.

Zweifach, A., and R.S. Lewis. 1993. Mitogen-regulated Ca^{2+} current of T lymphocytes is activated by depletion of intracellular stores. *Proc. Natl. Acad. Sci. USA.* 90:6295–6299.